

To Shuffle or not to Shuffle: Auditing DP-SGD with Shuffling

Meenatchi Sundaram Muthu Selva Annamalai¹, Borja Balle², Jamie Hayes², Emiliano De Cristofaro³

¹University College London ²Google DeepMind ³UC Riverside

Abstract

The Differentially Private Stochastic Gradient Descent (DP-SGD) algorithm allows the training of machine learning (ML) models with formal Differential Privacy (DP) guarantees. Since DP-SGD processes training data in batches, it employs Poisson sub-sampling to select each batch at every step. However, it has become common practice to replace sub-sampling with shuffling owing to better compatibility and computational overhead. At the same time, we do not know how to compute tight theoretical guarantees for shuffling; thus, DP guarantees of models privately trained with shuffling are often reported as though Poisson sub-sampling was used.

This prompts the need to verify whether gaps exist between the theoretical DP guarantees reported by state-of-the-art models and their actual leakage. To do so, we introduce a novel DP auditing procedure to analyze DP-SGD with shuffling and show that DP models trained with this approach have considerably overestimated privacy guarantees (up to 4 times). In the process, we assess the impact on privacy leakage of several parameters, including batch size, privacy budget, and threat model. Finally, we study two common variations of the shuffling procedure that result in even further privacy leakage (up to 10 times). Overall, our work attests to the risk of using shuffling instead of Poisson sub-sampling vis-à-vis privacy leakage from DP-SGD.

1 Introduction

Without robust privacy protections, Machine Learning (ML) models can be vulnerable to inference attacks exposing sensitive information about the training data [9, 51, 58]. To mitigate these risks, Differentially Private Stochastic Gradient Descent (DP-SGD) [1] can be used to train models with Differential Privacy [24] (DP) guarantees, which provably bounds the leakage from a model so that no adversary can confidently learn (up to a privacy parameter ϵ) any individual-level information about the training data. DP-SGD is supported by many open-source libraries [7, 31, 60] and is deployed in state-of-the-art (SOTA) private models with performance increasingly approaching that of non-private models [19].

DP-SGD with Shuffling. Since DP-SGD is computationally intensive, practitioners often attempt to optimize it. As DP-SGD processes training data in batches, the standard approach to select batches at each step is *Poisson sub-sampling*, which requires random access to the entire dataset and can be slow for large datasets [49]. As a result, recent work has begun to

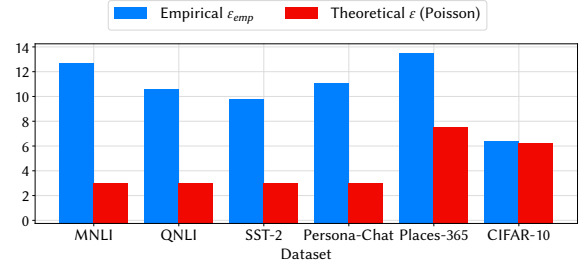


Figure 1: Largest gaps observed, for each dataset, between the empirical privacy leakage estimate ϵ_{emp} and theoretical Poisson guarantees ϵ when training by shuffling datasets using DP-SGD (in the Worst-Case threat model, 95% CI).

replace Poisson sub-sampling with *shuffling* the training data, and deterministically iterating over fixed-size batches [19, 50, 53]. An additional benefit is that modern ML pipelines (e.g., XLA compilation [47]) are optimized for fixed batch sizes, while Poisson sub-sampling produces different batch sizes, which can significantly slow down private training [13].

Motivation. Correctly estimating the theoretical guarantees provided by DP-SGD with shuffling remains an active area of research [16, 17, 30]. By contrast, the privacy analysis of Poisson sub-sampling is well-studied and admits strong privacy amplification [5, 22]. As a result, it is common for models using DP-SGD to be trained using shuffling, even though DP guarantees are reported as though Poisson sub-sampling was used [19, 40, 49], which prompts the need to analyze whether this affects the actual privacy leakage. In the rest of the paper, we use DP-SGD (Shuffle) to denote the former and DP-SGD (Poisson) for the latter.

Chua et al. [16, 17] recently discuss theoretical lower bounds for a simplified version of DP-SGD. They show that shuffling’s *lower bound* privacy analysis, in some settings, can be significantly larger than the expected *upper bounds* from Poisson sub-sampling. However, their lower bound analysis does not cover the gradient computation process of DP-SGD. Also, they do not evaluate parameter settings used in SOTA models using shuffling [19, 40]. Independently, shuffling inputs has also attracted strong interest in the “shuffle model” [8], with (nearly) tight guarantees given for pure DP mechanisms that use shuffling through third-party servers [6, 26, 27, 28, 55]. That said, we focus on DP-SGD in the “central model,” where shuffling is commonly used in practice. Consequently, verifying the technical validity of the DP guarantees of private ML models trained with shuffling remains an open research problem.

Roadmap. In this paper, we analyze the gap between the em-

empirical privacy leakage of DP-SGD (Shuffle) and the theoretical guarantees provided by DP-SGD (Poisson) vis-à-vis different capabilities and variations of the shuffling procedure. We do so using DP auditing [21], a technique that is increasingly used to estimate and compare the empirical privacy leakage from DP mechanisms against the theoretical DP upper bounds [2, 3, 11, 32, 33, 43, 44].

First, we define a simplified version of DP-SGD, which we denote as the “Batched Gaussian Mechanism” (BGM), and audit it using a novel method that builds on likelihood ratio functions. Our BGM variant is non-adaptive and simpler than the mechanism studied by Chua et al. [16], enabling us to audit it tightly in a principled way (see Section 3). Then, we extend our auditing procedure to DP-SGD (Shuffle) and evaluate the empirical privacy leakage under various threat models. We define increasingly powerful threat models, Natural, Partially-Informed, and Worst-Case, where the adversary can insert progressively more canary gradients and experiment with multiple datasets and common model architectures.

Although we focus on DP-SGD (Shuffle), our auditing framework is widely applicable to and can potentially be used with any sampling technique and mechanism. For instance, our auditing procedure can be used to identify variations within, and estimate privacy leakage for, implementations of shuffling itself.

Main Findings. Our experiments highlight a substantial gap (up to $4\times$) between the empirical privacy leakage observed from SOTA models [19, 40] and their claimed theoretical DP guarantees. In Figure 1, we summarize the largest gaps for each dataset we experiment with under the Worst-Case threat model. In the (relatively weaker) Partially-Informed model, we continue to observe DP violations from DP-SGD (Shuffle), especially for small batch sizes. For theoretical $\varepsilon = 1.0$, training a LeNet model on FMNIST with batch sizes of 100 and 1,000 yields empirical privacy leakage estimates of $\varepsilon_{emp} = 3.46$ and $\varepsilon_{emp} = 0.96$, respectively.

We also audit the privacy leakage from two variations of the shuffling procedure reported in prior work [49], i.e., partial shuffling and batch-then-shuffle. We find them in 2.6% of public code repositories related to non-private ML training and show that these variations yield even larger privacy leakage (up to $10\times$) compared to standard shuffling. For theoretical $\varepsilon = 0.1$, the partial shuffling and batch-then-shuffle procedures result in an empirical privacy leakage of $\varepsilon_{emp} = 0.29$ and $\varepsilon_{emp} = 1.00$, respectively.

Overall, while our experimental evaluation highlights gaps in privacy leakage that can often only be observed for small batch sizes and relatively strong threat models, we stress that DP should hold for all hyper-parameters and against worst-case adversaries.

Summary of Contributions:

- We present novel techniques to audit DP-SGD (Shuffle) using likelihood ratio functions, introducing a threat taxonomy specific to shuffling and adapting our auditing techniques accordingly.

- We are the first to audit DP-SGD (Shuffle) and to empirically show a substantial gap between the empirical privacy leakage observed from SOTA models [19, 40] and the theoretical DP guarantees, evaluating the impact of batch size and threat model on the empirical privacy leakage observed from DP-SGD (Shuffle).
- We investigate and find gaps in the privacy leakage from common variations to the shuffling procedure, namely, partial shuffling and batch-then-shuffle.
- Our work demonstrates the impact of shuffling and its variations on privacy leakage, calling into question the guarantees claimed by some SOTA models. This has important implications for the evaluation of models trained with DP-SGD (Shuffle) both in terms of privacy (i.e., privacy claims might be overly optimistic) and utility (i.e., hyper-parameters tuned to DP-SGD (Shuffle) may not be optimal for DP-SGD (Poisson) and vice-versa).

2 Background

2.1 Differential Privacy (DP)

Definition 2.1 (Differential Privacy (DP) [24]). *A randomized mechanism $\mathcal{M} : \mathcal{D} \rightarrow \mathcal{R}$ is (ε, δ) -differentially private if for any two adjacent datasets $D, D' \in \mathcal{D}$ and $S \subseteq \mathcal{R}$:*

$$\Pr[\mathcal{M}(D) \in S] \leq e^\varepsilon \Pr[\mathcal{M}(D') \in S] + \delta$$

The definition of adjacent (aka neighboring) datasets often varies depending on the setting. Two common adjacency notions are *add/remove* and *edit*. The former corresponds to inserting/deleting a single record from the dataset (hence $|D| = |D'| \pm 1$); the latter to replacing a single record with another ($|D| = |D'|$). The difference in the size of the adjacent datasets limits the applicability of the add/remove adjacency in some settings (e.g., sampling w/o replacement), while guarantees under edit adjacency typically require roughly twice the amount of noise [49] since replacing a record is equivalent to first deleting then adding a record under the add/remove adjacency.

Zero-out Adjacency. To bridge the gap between add/remove and edit adjacency, the “zero-out” adjacency [35] is increasingly used to simplify theoretical privacy analyses [14, 16, 49].

Definition 2.2 (Zero-out adjacency [35]). *Let \mathcal{X} be a data domain s.t. special element $\perp \notin \mathcal{X}$ and $\mathcal{X}_\perp = \mathcal{X} \cup \{\perp\}$. Datasets $D \in \mathcal{X}^n$ and $D' \in \mathcal{X}_\perp^n$ are zero-out adjacent if exactly one record in D is replaced with \perp in D' .*

The special \perp record is usually 0 for numerical data. This allows the guarantees under zero-out adjacency to be semantically equivalent to those under add/remove (i.e., no additional noise required) while ensuring that the sizes of the adjacent datasets are equal.

f -DP and trade-off functions. Besides (ε, δ) -DP, there are other formalizations of DP; e.g., f -DP captures the difficulty for

any adversary to distinguish between the outputs of a mechanism \mathcal{M} on adjacent datasets D and D' using trade-off functions.

Definition 2.3 (Trade-off function [22]). *For any two probability distributions P and Q on the same space, the trade-off function $T(P, Q) : [0, 1] \rightarrow [0, 1]$ is defined as:*

$$T(P, Q)(\alpha) = \inf\{\beta_\phi : \alpha_\phi \leq \alpha\}$$

where the infimum is taken over all (measurable) rejection rules ϕ and α_ϕ and β_ϕ are the type I and II errors corresponding to this rejection rule, respectively.

In theory, the trade-off function characterizes the false positive/negative errors achievable by any adversary aiming to distinguish between P and Q . A mechanism \mathcal{M} is said to satisfy f -DP if for all adjacent datasets D, D' : $T(\mathcal{M}(D), \mathcal{M}(D')) \geq f$.

One special case of f -DP is μ -GDP, when the underlying distributions are Gaussian.

Definition 2.4 (μ -GDP [22]). *A mechanism \mathcal{M} satisfies μ -GDP if for all adjacent datasets D, D' :*

$$T(\mathcal{M}(D), \mathcal{M}(D')) \geq \Phi(\Phi^{-1}(1 - \alpha) - \mu)$$

where Φ is the standard normal cumulative distribution function.

f -DP is useful, e.g., in the context of auditing (introduced in Section 3), as it is equivalent to (ϵ, δ) -DP for specific trade-off functions and can be used to efficiently compare the empirical power of adversaries with theoretical guarantees, as we do later in the paper.

Privacy Loss Distribution (PLD). The PLD formalism [37] is a useful technique first proposed to derive tight theoretical guarantees for DP mechanisms. In recent work [43], PLD has also been used to tightly audit DP-SGD (Poisson) by using the given PLD to estimate the corresponding trade-off function. However, while the PLD for DP-SGD (Poisson) is known, deriving the PLD for DP-SGD (Shuffle) is still an active area of research [16, 17].

2.2 DP-SGD

Differentially Private Stochastic Gradient Descent (DP-SGD) [1] is a popular algorithm for training machine learning (ML) models with formal privacy guarantees. DP-SGD takes in input a dataset D along with several hyper-parameters and proceeds iteratively, processing the dataset in batches and computing the gradients of samples one batch at a time. There are many strategies for sampling a batch from a dataset, e.g., Poisson sub-sampling, sampling without replacement, etc. Therefore, in general, DP-SGD can be defined with an abstract batch sampler \mathcal{B} that takes in as input the dataset D and the (expected) batch size B and outputs batches sampled from the dataset. We report its pseudo-code in Algorithm 3 in Appendix A.

Poisson Sub-Sampling. The first implementations of DP-SGD used batches sampled through Poisson sub-sampling. With this approach, the batch sampler independently samples each record $(x, y) \in D$ with probability $q = B/|D|$ in each batch, where B is the batch size. One major advantage of using Poisson sub-sampling is substantially reducing the amount of required noise via strong privacy amplification theorems [1, 22].

However, in practice, Poisson sub-sampling can be quite inefficient. For instance, the dataset cannot be fully loaded in memory when it is too large; thus, one needs to load a random batch in and out from the disk at every step, which is costly [49]. Furthermore, efficient modern ML pipelines (e.g., XLA compilation) require fixed-size batches to fully leverage GPU parallelization [13].

Shuffling. In practice, state-of-the-art DP-SGD implementations often rely on more computationally efficient sampling schemes, such as shuffling, while reporting DP guarantees as though Poisson sub-sampling was used [19]. In shuffling, the batch sampler randomly permutes the records first, then partitions the dataset into fixed-size batches. Since shuffling is already the standard in non-private training, this also simplifies implementations of DP-SGD by layering DP on top of existing non-private pipelines instead of redesigning and optimizing them from scratch. However, since the privacy guarantees provided by shuffling are not yet fully understood, this can create a discrepancy between the theoretical guarantees reported by state-of-the-art models and the actual privacy leakage, which we study in this work.

Zero-out Adjacency. While shuffling is more compatible with edit adjacency due to the fixed batch sizes, the Poisson scheme is more suitable for add/remove adjacency. Nevertheless, it is possible to derive guarantees for Poisson under the edit adjacency, although this is known to be very cumbersome [5]. Thus, comparing privacy guarantees between the different sub-sampling schemes is inherently complicated. Overall, zero-out adjacency is increasingly used to analyze the privacy of DP-SGD in practice [14, 35, 49].

Specifically, the \perp record is defined so that the gradient is always zero, i.e., $\forall \theta \nabla \ell(\perp; \theta) = \mathbf{0}$ [35]. By doing so, we ensure that DP-SGD (Poisson) under zero-out adjacency is semantically equivalent to DP-SGD (Poisson) under add/remove, which enables us to compare the privacy guarantees of DP-SGD (Poisson) with that of DP-SGD (Shuffle) under a common adjacency notion.

3 DP Auditing

Privacy auditing broadly denotes the process of empirically estimating the privacy leakage from an algorithm. In DP, this typically involves experiments to estimate the empirical privacy guarantees, denoted as ϵ_{emp} , and compare them to the claimed theoretical guarantees (ϵ). For simplicity, we assume the empirical privacy guarantees are derived for the same δ as the claimed theoretical (ϵ, δ) -DP. Therefore, we are technically

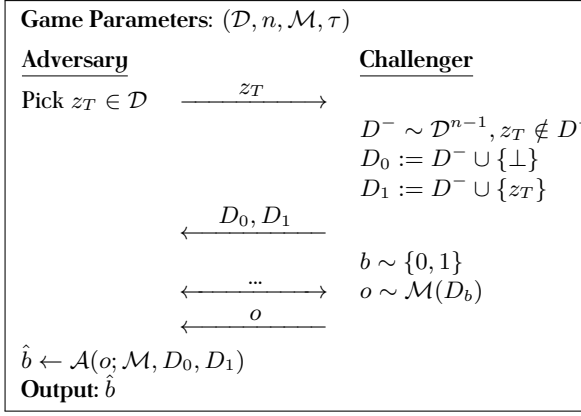


Figure 2: Distinguishability Game between an Adversary and a Challenger for zero-out DP given data distribution \mathcal{D} of size n , the mechanism \mathcal{M} , and a decision threshold τ .

comparing $(\varepsilon_{emp}, \delta)$ with (ε, δ) , but leave out δ throughout the paper to ease presentation.

If $\varepsilon_{emp} > \varepsilon$, the mechanism leaks more privacy than expected; whereas if $\varepsilon_{emp} \ll \varepsilon$, the theoretical bounds may be loose, or there may be substantial room for improvement to the privacy estimation procedure—i.e., the audit is not *tight*. Empirical guarantees are also useful for estimating the privacy loss in settings where tight theoretical guarantees are not currently known, e.g., when the adversary does not have access to intermediate updates [2, 3].

Implementing DP algorithms correctly is notoriously challenging [10, 34] and bugs in DP-SGD implementations have resulted in significantly degraded protections [11, 34] and realistic privacy attacks [20]. DP auditing can be used to detect these bugs [4, 43, 54] as well as to evaluate the optimality of privacy attacks [4, 44].

In this work, we present auditing techniques to empirically estimate the privacy loss of DP-SGD (Shuffle). By comparing it with the theoretical guarantees of DP-SGD (Poisson), we evaluate the impact of using shuffling instead of Poisson sub-sampling on the privacy leakage of DP-SGD. In the rest of this section, we introduce a general auditing procedure using an adversary and a distinguishing game. The attack’s success can then be converted into the lower-bound empirical privacy leakage estimate ε_{emp} .

3.1 The Distinguishing Game

In Figure 2, we formalize the distinguishing game, involving an Adversary and a Challenger, used to audit the zero-out DP guarantees of a mechanism \mathcal{M} . The Challenger runs the mechanism on a randomly chosen dataset, and the Adversary aims to determine the dataset used by the Challenger based on the mechanism’s output.

In each game, the Adversary picks a single target record z_T from the data domain (we slightly abuse notation and define \mathcal{D} as both the data *distribution* and *domain*) and sends it to the Challenger. This constructs adjacent datasets D_0 and D_1 by appending the zero-out record \perp and the target record z_T , respectively, to a randomly sampled dataset with $n - 1$

records. In prior work, stronger adversarial settings where the Adversary also chooses adjacent datasets D_0 and D_1 directly have also been considered [4, 44]. However, in the context of DP-SGD, adversarial datasets can destroy model utility and represent an unrealistic adversarial setting [43, 44]. Therefore, in our work, we consider randomly crafted datasets to estimate the empirical privacy leakage in more real-world settings [2, 43, 48, 52]. Thus, the Adversary is given access to the randomly sampled adjacent datasets D_0 and D_1 .

Next, the Challenger runs \mathcal{M} on dataset D_b for a random $b \in \{0, 1\}$. Note that \mathcal{M} can be a complex algorithm with many implementation details that the theoretical privacy analysis does not rely on; thus, depending on the threat model considered and the adversarial capabilities, the adversary may be given access to specific internals of \mathcal{M} as discussed in Section 5.1, along with \mathcal{M} ’s output. In theory, this can take any form, e.g., scalar $o \in \mathbb{R}$, vector $o \in \mathbb{R}^d$, or even have arbitrary domain $o \in \mathcal{Y}$. However, it can be difficult to consider and design decision functions around values in arbitrary domains. Hence, a common strategy [32, 44] is for the Adversary to define a distinguishing function \mathcal{A} that assigns a scalar “score” to the output representing the Adversary’s confidence that the output is drawn from processing D_1 . This score is then thresholded to produce a guess $\hat{b} = 1$ if the Adversary determines that $o \sim \mathcal{M}(D_1)$ and 0 otherwise. The adversary wins the game if $\hat{b} = b$.

3.2 Estimating ε_{emp}

We estimate the empirical privacy leakage ε_{emp} by running the distinguishing game multiple times, where only a single record is inserted in each run. (This is different from recent “auditing in one run” methods [42, 52, 56], which we do not use as these do not yield sufficiently tight audits of DP-SGD even under powerful threat models.) Specifically, we compute the false positive rate (FPR) α and the false negative rate (FNR) β across multiple games and derive (statistically valid) upper bounds $\bar{\alpha}$ and $\bar{\beta}$ using Clopper-Pearson confidence intervals (CIs) to quantify the confidence in our privacy loss estimation [32, 43]. We then calculate the empirical lower-bound privacy guarantee ε_{emp} from $\bar{\alpha}$ and $\bar{\beta}$ using the (ε, δ) -DP definition as follows.

Although recent work [42, 43, 56] has proposed more advanced auditing techniques for DP-SGD (Poisson) using f -DP or PLD, since tighter f -DP guarantees for DP-SGD (Shuffle) are currently unknown [16], we stick to the (ε, δ) -DP definition.

Auditing using (ε, δ) -DP. For any given (ε, δ) -DP mechanism, the possible false positive rates (α) and false negative rates (β) attainable by any adversary are known to be the following privacy region [36]:

$$\mathcal{R}(\varepsilon, \delta) = \{(\alpha, \beta) \mid \alpha + e^\varepsilon \beta \geq 1 - \delta \wedge e^\varepsilon \alpha + \beta \geq 1 - \delta \wedge \alpha + e^\varepsilon \beta \leq e^\varepsilon + \delta \wedge e^\varepsilon \alpha + \beta \leq e^\varepsilon + \delta\}$$

Therefore, given upper bounds $\bar{\alpha}$ and $\bar{\beta}$, the empirical lower

bound can be calculated as:

$$\varepsilon_{emp} = \max \left\{ \ln \left(\frac{1 - \bar{\alpha} - \delta}{\bar{\beta}} \right), \ln \left(\frac{1 - \bar{\beta} - \delta}{\bar{\alpha}} \right), 0 \right\} \quad (1)$$

While Bayesian intervals [61] can improve the privacy estimation’s tightness, they are also more computationally expensive to derive and may not always be statistically sound [43]. Thus, we stick to Clopper-Pearson CIs. (Later in the paper, we will also evaluate the impact of using CIs on the empirical privacy leakage estimation).

For simplicity, we follow standard practice [32, 43, 52, 61] and fix the value of $\delta = 10^{-5}$ throughout all experiments and only estimate the ε_{emp} guarantee at this δ value.

3.3 The Distinguishing Function

As discussed above, DP auditing involves an adversary distinguishing between observations from $\mathcal{M}(D)$ and $\mathcal{M}(D')$. For a mechanism $\mathcal{M} : \mathcal{X} \rightarrow \mathcal{Y}$, this can be any function of the form $\mathcal{A} : \mathcal{Y} \rightarrow \{0, 1\}$ where $\mathcal{A}(o) = 1$ (or 0) represents that the adversary predicts that the observation o is drawn from $\mathcal{M}(D)$ (or $\mathcal{M}(D')$).

Scalar Score. In theory, \mathcal{A} is equivalent to the rejection rule from the definition of f -DP, which represents the adversary performing a hypothesis test on whether to reject that $o \sim \mathcal{M}(D')$. However, in previous work [32, 33, 43, 44], the adversary assigns a scalar “score” to each output, which is then thresholded to form the distinguishing function—e.g., Jagielski et al. [32] and Nasr et al. [43] use the loss function and dot product, respectively. This is because the raw outputs of DP-SGD tend to be high-dimensional vectors where distances can be difficult to interpret, thus making distinguishing functions hard to design.

On the other hand, using a scalar score, the adversary can first represent the *confidence* that the observation was drawn from $\mathcal{M}(D)$ instead of $\mathcal{M}(D')$. Then, the score can be thresholded to produce a prediction easily, i.e., all observations with score $\geq \tau$ are labeled as drawn from $\mathcal{M}(D)$ and from $\mathcal{M}(D')$ otherwise. Furthermore, this threshold τ can also be adjusted to produce not only a single FPR/FNR pair but an FPR-FNR curve, i.e., an empirical *trade-off curve*, which can also be compared with the claimed theoretical trade-off function when auditing.

Choosing the threshold. When auditing using scalar scores, choosing the threshold τ from an independent set of observations is the easiest method to ensure a technically valid lower bound for the empirical privacy leakage estimate ε_{emp} derived this way. However, it is standard to report the maximum ε_{emp} for the optimal threshold [3, 11, 32, 43, 44, 48, 61] and we do so too, making the process more efficient by first sorting the scalar scores. For simplicity, we abstract the details of choosing an appropriate threshold and designing a distinguishing function. We refer to the empirical estimation procedure at significance level α and privacy parameter δ from scores \mathcal{S} and \mathcal{S}' derived from $\mathcal{M}(D)$ and $\mathcal{M}(D')$, respectively as $\text{EstimateEps}(\mathcal{S}, \mathcal{S}', \alpha, \delta)$ – see Appendix B for more details.

4 Warm Up: Auditing the Batched Gaussian Mechanism

Before auditing DP-SGD, we start with the Batched Gaussian Mechanism (BGM) (reviewed in Algorithm 4 in Appendix A), a heavily simplified version of DP-SGD adapted from [16] to develop principled tight auditing techniques for shuffling under an idealized setting. Similar to DP-SGD, BGM also proceeds iteratively, sampling batches according to some batch sampler \mathcal{B} . However, instead of calculating gradients, the inputs are simply aggregated together with noise at each batch, and the noisy aggregated values are released for each batch across all epochs. Also, unlike DP-SGD, it is *non-adaptive*, i.e., the outputs of previous iterations do not affect the current one.

Although BGM can be instantiated with any batch sampler, we use the shuffle batch sampler, which is commonly used in ML training. We bound the inputs, i.e. $\forall i \ x_i \in [-1, +1]$, so that the mechanism satisfies (ε, δ) -DP. When the number of epochs is 1, Chua et al. [16] use the adjacent datasets $D = (+1, -1, \dots, -1)$ and $D' = (\perp, -1, \dots, -1)$, setting $\perp = 0$ in their lower bound privacy analysis. Specifically, they conjecture, but do not prove, that these are the worst-case adjacent datasets for the shuffle batch sampler. Note that this is different from the proven worst-case datasets $D = (+1, 0, \dots, 0)$ and $D' = (\perp, 0, \dots, 0)$ for the Poisson batch sampler [62]. Specifically, in the shuffle setting, the differing sample in the conjectured worst-case datasets is equal in magnitude but opposite in direction to the other samples unlike in the Poisson setting. Finally, in a single epoch and for batch size B , the outputs of the mechanism on the adjacent datasets are $(-B, \dots, -B + 2, \dots, -B) + \mathcal{N}(0, \sigma^2 \mathbb{I})$ and $(-B, \dots, -B + 1, \dots, -B) + \mathcal{N}(0, \sigma^2 \mathbb{I})$ for D and D' , respectively. Since the inputs are shuffled, the “ $-B+2$ ” and “ $-B+1$ ” values can appear in any batch.

Unlike DP-SGD, BGM is a hypothetical algorithm that is not already associated with common “data distributions” (e.g., training datasets). Therefore, when auditing BGM using the Distinguishability Game described earlier, we take the data distribution to be the “pathological” distribution, which always outputs ‘-1.’ Then, the adversary always chooses ‘+1’ as the target record z_T .

4.1 Single Epoch

To audit a single epoch, an adversary has to distinguish between the outputs $(\tilde{g}_1, \dots, \tilde{g}_T) \sim \text{BGM}(D)$ and $(\tilde{g}'_1, \dots, \tilde{g}'_T) \sim \text{BGM}(D')$. As mentioned, prior DP-SGD audits typically compute a natural “score” from each thresholded observation. However, in the context of shuffling, there is no known score to distinguish between the outputs.

In this work, we draw from the Neyman-Pearson [46] lemma, which states that the optimal way to distinguish between two distributions is by thresholding the output of the *likelihood ratio* function. Specifically, the likelihood ratio function computes the ratio of probabilities that the outputs are from $\text{BGM}(D)$ or $\text{BGM}(D')$. Here, the probability that $(\tilde{g}_1, \dots, \tilde{g}_T)$ is from $\text{BGM}(D)$ (or $\text{BGM}(D')$) can be split into

T cases depending on which batch the target record $+1$ (or \perp) appears in. To that end, we calculate the likelihood ratio for the adjacent datasets $D = (+1, -1, \dots, -1)$ and $D' = (\perp, -1, \dots, -1)$ as follows (we let $\tilde{\mathbf{g}} = (\tilde{g}_1, \dots, \tilde{g}_T)$):

$$\Lambda(\tilde{\mathbf{g}}) = \frac{\Pr[\tilde{\mathbf{g}}|\text{BGM}(D)]}{\Pr[\tilde{\mathbf{g}}|\text{BGM}(D')]} = \frac{\sum_t T^{-1} \Pr[\tilde{\mathbf{g}}|\text{BGM}(D) \wedge +1 \text{ is in batch } t]}{\sum_t T^{-1} \Pr[\tilde{\mathbf{g}}|\text{BGM}(D') \wedge \perp \text{ is in batch } t]} \\ = \frac{\sum_t \Pr[\tilde{g}_t|\mathcal{N}(-B+2, \sigma^2)] \prod_{t' \neq t} \Pr[\tilde{g}_{t'}|\mathcal{N}(-B, \sigma^2)]}{\sum_t \Pr[\tilde{g}_t|\mathcal{N}(-B+1, \sigma^2)] \prod_{t' \neq t} \Pr[\tilde{g}_{t'}|\mathcal{N}(-B, \sigma^2)]}$$

Note that for arbitrary adjacent datasets where all records are different, $\Lambda(\cdot)$ would be computationally intractable to compute since we would need to account for all possible permutations induced by shuffling. However, since [16]’s conjecture assumes that all records except one are identical, this reduces the number of “cases” to be considered to T , thus making $\Lambda(\cdot)$ tractable.

4.2 Multiple Epochs

Although [16] only considers one set of batches (i.e., corresponding to a single “epoch” of training), we extend to multiple epochs as training private models typically involves training across multiple epochs. We rely on the fact that the batch sampling and aggregation are done *independently* across multiple epochs, thus, the likelihood across multiple epochs is the prod-

uct of the likelihoods of each epoch, i.e., letting $\mathcal{G} = \begin{bmatrix} -\tilde{\mathbf{g}}^1 - \\ \vdots \\ -\tilde{\mathbf{g}}^E - \end{bmatrix}$,

we define the likelihood ratio as:

$$\Lambda^{\text{BGM}}(\mathcal{G}) = \prod_{i=1}^E \Lambda(\tilde{\mathbf{g}}^i) = \\ = \prod_{i=1}^E \frac{\sum_t \Pr[\tilde{g}_t^i|\mathcal{N}(-B+2, \sigma^2)] \prod_{t' \neq t} \Pr[\tilde{g}_{t'}^i|\mathcal{N}(-B, \sigma^2)]}{\sum_t \Pr[\tilde{g}_t^i|\mathcal{N}(-B+1, \sigma^2)] \prod_{t' \neq t} \Pr[\tilde{g}_{t'}^i|\mathcal{N}(-B, \sigma^2)]}$$

Overall, our experimental evaluation (in Section 6.2) will show that auditing using likelihood ratios is very effective at estimating the privacy leakage from the Batched Gaussian Mechanism. In this idealized setting, we observe a substantial gap (up to $4\times$) between the empirical privacy leakage observed and the theoretical guarantees produced by the Poisson sub-sampling analysis (recall that there are no known guarantees for shuffling). This prompts the need to investigate whether such a gap is also observable in more real-world settings using DP-SGD.

Our auditing techniques can be easily extended, as done above, by simply defining the appropriate likelihood ratio function. In the rest of the paper, we rely on this extensibility to audit the DP-SGD (Shuffle) implementation under varying threat models and audit implementations with variations in the shuffling procedure.

5 Auditing DP-SGD (Shuffle)

In this section, we extend the auditing procedure from the Batched Gaussian Mechanism to DP-SGD (Shuffle). We start

by defining various threat models specific to the shuffling setting and then present our auditing procedure.

5.1 Threat Models

Although DP-SGD (Shuffle)’s structure is very similar to that of the Batched Gaussian Mechanism, there are practical considerations that can affect the empirical privacy estimates. For instance, since the inputs to the mechanism are directly aggregated and all intermediate noisy aggregates are released, adversaries for the Batched Gaussian Mechanism are, by default, given as much power as the theoretical worst-case DP adversary. By contrast, DP-SGD first calculates the gradient of each input before aggregating them and may only output the final trained model, thus making it unclear which aspects of the mechanism potential real-world adversaries would be given access to.

Theoretically, the worst-case adversary assumed by the DP guarantees has access to all aspects of the algorithm not involved in the randomness for noise addition and batch selection. Nevertheless, we believe it is interesting to relax this assumption and explore how varying the adversary’s capabilities can affect the empirical privacy leakage that is achievable in practice as done in prior work [3, 32, 43, 44, 52]. Specifically, prior work has considered several threat models (e.g., “input-space” vs. “gradient-space” [43, 52], “white-box” vs. “black-box” [3, 32, 44]) and assess their impact of the empirical privacy leakage in the context of Poisson sub-sampling. However, these threat models may not necessarily capture the range of capabilities an adversary can possess in the context of shuffling.

Overall, adversaries used for DP auditing are usually given relatively strong assumptions. In our work, we consider adversaries with (active) white-box access to the model, aka “white-box with gradient canaries,” as done in early DP-SGD audits [43, 44]. First, the adversary can choose the target record (\hat{x}, \hat{y}) . Next, they have access to the model parameters at each update step and can arbitrarily insert gradients of samples (i.e., gradient canary). Finally, as we focus on auditing DP-SGD (Shuffle) in real-world settings, we assume that the adversary cannot craft a pathological dataset [44] but is instead only given access to real-world datasets (e.g., CIFAR-10). Given the “base” adversarial capabilities described above, we then vary the threat model by limiting the number of gradients the adversary can insert. Specifically, we consider three main threat models with increasing adversarial capabilities, namely, Natural, Partially-Informed, and Worst-Case.

Natural. This corresponds to the model originally defined in [43], where an adversary can only insert the gradient of the target record. Specifically, all other records have natural (not adversarially crafted) gradients. In practice, we expect models audited under this threat model to have the same utility as production models, as the canary gradient has minimal impact on it. Although this setting produces tight estimates for DP-SGD (Poisson) [43], our experiments show that it can heavily underestimate the empirical privacy leakage of DP-SGD (Shuffle) – see Section 6.3.3 – thus motivating us to consider stronger

threat models.

Partially-Informed. Next, we consider a slightly stronger adversary that can insert the gradients of the target record and the final record in each batch. While under Natural, the adversary only inserts one gradient (for the target record) across all batches, here we assume they can insert one gradient for *each batch* while leaving those of the remaining $B-1$ samples untouched. This threat model serves as a hypothetical middle-ground between our strongest and weakest threat model and in practice, allows the adversary to identify the batch containing the target or zero-out record with higher precision, which in turn translates to significantly larger empirical privacy leakage estimates. Since the gradient inserted is typically very small compared to the gradients of the normal samples, models audited under this threat model should still maintain similar utilities as production models.

Worst-Case. Finally, we consider an adversary that can insert the gradients of all records in the dataset. This corresponds to auditing the Batched Gaussian Mechanism. Although this may be unrealistic and completely destroy model utility, we emphasize that DP guarantees should hold against the most powerful adversary, which this threat model corresponds to. Thus, it is at least useful to evaluate the maximum empirical privacy leakage possible.

5.2 Auditing Procedure

In Algorithm 1, we outline the DP-SGD algorithm [1] with the modifications needed to audit under Natural and Partially-Informed reported in red and, in blue only for the latter. Since Worst-Case is equivalent to auditing BGM, for the sake of efficiency, experiments in this threat model directly audit BGM.

Lines 7-8 correspond to enforcing that the \perp record has a 0 gradient, which is necessary for auditing with zero-out adjacent datasets. Furthermore, lines 9-10 are standard for active white-box adversaries that insert the gradient of the target record.

Lines 11-12 correspond to inserting the gradient of the final record in each batch, which is only executed under Partially-Informed (and not Natural); specifically, the adversary inserts the canary gradient in the opposite direction for each batch that does not contain both the target and zero-out record. Recall that this closely resembles the conjectured worst-case datasets by Chua et al. [16] as the target record's gradient has an equivalent magnitude but opposite direction to the final records in all other batches, which makes audits under this threat model tighter. This does not break or change the underlying DP guarantees of DP-SGD (Shuffle) as this step is applied regardless of whether the target or zero-out record is present in the dataset and thus applies to D and D' equally.

Finally, all adversaries compute the dot product between the privatized and canary gradient as “outputs” (line 20) and release the full matrix of “outputs” across all batches and epochs (line 23). Similar to the Batched Gaussian Mechanism, the adversary computes and thresholds the likelihood ratio to calculate empirical privacy leakage estimates.

Algorithm 1 DP-SGD (Audit). Modifications needed to audit under the Natural and Partially-Informed threat models are reported in red. Modifications in blue are additionally added under the Partially-Informed threat model.

Require: Dataset, D . Epochs, E . Batch Size, B . Learning rate, η . Batch sampler, \mathcal{B} . Loss function, ℓ . Initial model parameters, θ_0 . Noise multiplier, σ . Clipping norm, C . **Target record**, (\hat{x}, \hat{y}) . **Canary gradient**, \hat{g} . **Zero-out record**, (x_\perp, y_\perp) .

```

1:  $T \leftarrow |D|/B$ 
2: for  $i \in [E]$  do
3:    $\theta_1^i \leftarrow \theta_T^{i-1}$ 
4:   Sample batches  $B_1, \dots, B_T \leftarrow \mathcal{B}(D, B)$ 
5:   for  $t \in [T]$  do
6:     for  $(x_j, y_j) \in B_t$  do
7:       if  $(x_i, y_i) = (x_\perp, y_\perp)$  then
8:          $g_j \leftarrow \mathbf{0}$ 
9:       else if  $(x_j, y_j) = (\hat{x}, \hat{y})$  then
10:         $g_j \leftarrow \hat{g}$ 
11:      else if  $j = B - 1 \wedge (\hat{x}, \hat{y}), (x_\perp, y_\perp) \notin B_t$  then
12:         $g_j \leftarrow -\hat{g}$ 
13:      else
14:         $g_j \leftarrow \nabla \ell((x_j, y_j); \theta_t^i)$ 
15:         $\bar{g}_j \leftarrow g_j / \max\left(1, \frac{\|g_j\|_2}{C}\right)$ 
16:       $\tilde{g} \leftarrow \frac{1}{B} \left( \sum_j \bar{g}_j + \mathcal{N}(0, C^2 \sigma^2 \mathbb{I}) \right)$ 
17:       $\theta_{t+1}^i \leftarrow \theta_t^i - \eta \tilde{g}$ 
18:       $o_t^i \leftarrow \langle \tilde{g}, \hat{g} \rangle$ 
19: return  $\mathcal{O} = \begin{bmatrix} o_1^1 & \dots & o_T^1 \\ \vdots & \ddots & \vdots \\ o_1^E & \dots & o_T^E \end{bmatrix}$ 

```

In our auditing procedure, the adversary does not have access to the underlying batch sampler \mathcal{B} , but only to the output matrix \mathcal{O} . We do so as we focus on determining the impact of alternate sub-sampling schemes on the empirical privacy leakage. This allows us not only to assess whether the adversary can leak more privacy without knowing the specifications of the batch sampler but also to detect bugs within the shuffling implementations (see Section 7).

Overall, our auditing procedure assumes an adversary that can access all parts of training other than the clipping, noise addition, and batch selection steps and is only slightly weaker than the adversary assumed by DP-SGD's privacy analysis (i.e., the optimal adversary can also choose a pathological dataset D and has access to the batch sampler).

5.3 Computing Likelihood Ratios

Lastly, similar to the BGM audit presented above, the adversary calculates the score assigned to the mechanism's output using the Neyman-Pearson lemma. While this is similar to the BGM setting, the likelihood ratios differ slightly depending on the threat model. Mainly, $o_t^i = \langle \tilde{g}, \hat{g} \rangle \approx 0$ if \hat{g} or $-\hat{g}$ were not inserted by the adversary in Steps 10 or 12 and $o_t^i \approx +1$ and ≈ -1 , respectively, otherwise. For each threat model, we calculate $\Lambda(\mathcal{O})$ as follows.

- Natural (Λ^N):

$$\prod_{i=1}^E \frac{\sum_t \Pr[o_t^i | \mathcal{N}(+1, \sigma^2)] \prod_{t' \neq t} \Pr[o_{t'}^i | \mathcal{N}(0, \sigma^2)]}{\prod_t \Pr[o_t^i | \mathcal{N}(0, \sigma^2)]}$$

- Partially-Informed (Λ^{PI}):

$$\prod_{i=1}^E \frac{\sum_t \Pr[o_t^i | \mathcal{N}(+1, \sigma^2)] \prod_{t' \neq t} \Pr[o_{t'}^i | \mathcal{N}(-1, \sigma^2)]}{\sum_t \Pr[o_t^i | \mathcal{N}(0, \sigma^2)] \prod_{t' \neq t} \Pr[o_{t'}^i | \mathcal{N}(-1, \sigma^2)]}$$

- Worst-Case (Λ^{WC}):

$$\prod_{i=1}^E \frac{\sum_t \Pr[o_t^i | \mathcal{N}(-B+2, \sigma^2)] \prod_{t' \neq t} \Pr[o_{t'}^i | \mathcal{N}(-B, \sigma^2)]}{\sum_t \Pr[o_t^i | \mathcal{N}(-B+1, \sigma^2)] \prod_{t' \neq t} \Pr[o_{t'}^i | \mathcal{N}(-B, \sigma^2)]}$$

6 Experimental Evaluation

In this section, we present our experimental evaluation to compare the empirical privacy leakage observed from mechanisms that use shuffling (ε_{emp}) with the upper-bound privacy leakage guaranteed by the analysis using Poisson sub-sampling (ε).

We first audit the Batched Gaussian Mechanism (BGM) over various parameters before moving on to auditing the DP-SGD (Shuffle) algorithm. In the process, we also evaluate the impact of several key factors, such as batch size and adversarial capabilities, on the empirical privacy leakage.

6.1 Experimental Setup

Across all experiments, we report lower bounds with 95% confidence (Clopper-Pearson [18]) along with the mean and standard deviation values of ε_{emp} over five independent runs. For simplicity, in all experiments, we set $\delta = 10^{-5}$, gradient clipping norm to $C = 1.0$, and choose the learning rate η by hyper-parameter tuning from a logarithmic scale.

Datasets. We use three datasets commonly used in the DP auditing literature, namely, FMNIST [57], CIFAR-10 [38], and Purchase-100 (P100) [51]. Due to computational constraints, we only take samples corresponding to two labels from FMNIST and CIFAR-10 and downsample all datasets only to include 10,000 samples as also done in prior work [32]. Our FMNIST dataset contains 10,000 28x28 grayscale images from one of two classes (‘T-shirt’ and ‘Trouser’), while our CIFAR-10 dataset contains 10,000 3x32x32 RGB images from one of two classes (‘Airplane’ and ‘Automobile’). Finally, our P100 dataset consists of 10,000 records with 600 binary features from one of a hundred classes.

Models. For CIFAR-10, we train a moderate-sized Convolutional Neural Network (CNN) drawn from prior work [23]. For FMNIST and P100, we train a small LeNet and an MLP model, respectively. We refer to Appendix C for more details on the model architectures.

Experimental Testbed. We run all experiments on a cluster using 4 NVIDIA A100 GPUs, 64 CPU cores, and 100GB RAM. Auditing a single model using 10^6 observations took 38.8, 17.1, and 5.70 hours for the shallow CNN, LeNet, and MLP models, respectively.

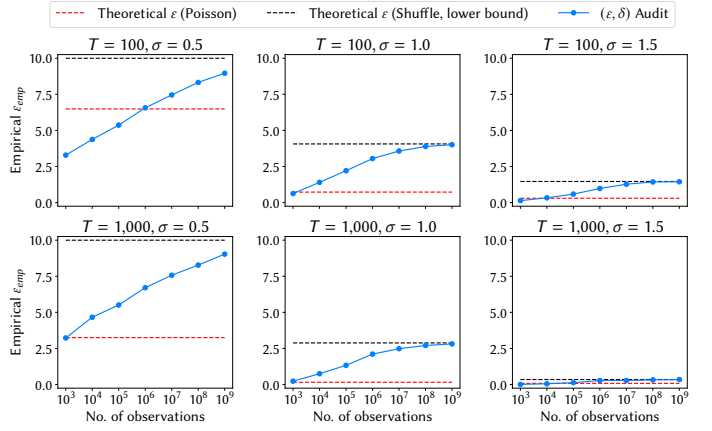


Figure 3: Auditing BGM for various number of steps T and noise multipliers σ . Theoretical ε (Poisson) represents the theoretical guarantees if Poisson sub-sampling had been used, while Theoretical ε (Shuffle, lower bound) denotes the lower bounds from [16].

6.2 Auditing the Batched Gaussian Mechanism

We audit BGM using the procedure outlined in Section 4 with varying batch sizes, B , and noise multipliers, σ .

6.2.1 Varying batch size and noise multiplier

We start by fixing both the number of epochs and the batch size to 1. Then, we vary the *number of steps* for a single epoch, T , by varying the dataset size and can then compute the theoretical Poisson analysis ε using the privacy loss random variable (PRV) accountant for a given T and noise multiplier σ . Furthermore, in order to analyze the computational requirements for running our audits, we audit each setting over a varying number of runs of the game, each yielding a single observation. For context, we also consider the lower bound theoretical ε previously calculated by Chua et al. [16].

In Figure 3, we plot the empirical ε_{emp} observed when auditing the Batched Gaussian Mechanism with the numbers of steps T at 100 and 1,000 and noise multipliers σ at 0.5, 1.0, 1.5. For several parameters, the empirical privacy leakage is substantially larger than the theoretical upper bounds from the Poisson analysis. Specifically, with $T = 100$, we obtain $\varepsilon_{emp} = 8.96, 4.01$, and 1.44 , respectively, for $\sigma = 0.5, 1.0, 1.5$ against theoretical upper bounds suggesting only $\varepsilon = 6.49, 0.73, 0.30$ (over 10^9 observations).

This gap varies with different numbers of steps taken in each epoch (T) and different noise multipliers (σ). More precisely, it is substantially larger for larger T (corresponding to small batch sizes) and smaller σ . For instance, the gap between ε and ε_{emp} is 5.78 for $T = 1000, \sigma = 0.5$ vs. 1.14 for $T = 100, \sigma = 1.5$. However, larger numbers of steps may not always result in larger empirical privacy leakage estimates either. At $\sigma = 1.5$, for $T = 100$ and 1000, we find $\varepsilon_{emp} = 1.44$ and $\varepsilon_{emp} = 0.34$, respectively.

Since we are auditing using the (ε, δ) -DP definition, we need a large number of observations for the ε_{emp} estimates to converge, especially with small σ . For $\sigma \geq 1.0$, at $T = 100$, ε_{emp} converges after 10^8 observations but, for $\sigma = 0.5$, it re-

Paper	Dataset	σ	T	E	ϵ	ϵ_{emp}	Gap
[19]	Places-365	1.00	440	509	7.53	13.54	$1.80\times$
[19]	CIFAR-10	3.00	11	168	6.24	6.39	$1.02\times$
[40]	SST-2	0.79	117	10	3.00	9.80	$3.27\times$
[40]	QNLI	0.87	195	30	3.00	10.60	$3.53\times$
[40]	MNLI	0.73	781	50	3.00	12.73	$4.25\times$
[40]	Persona-Chat	0.82	254	30	2.99	11.08	$3.70\times$

Table 1: Real-world parameter settings where the empirical privacy leakage (ϵ_{emp}) observed from shuffling is appreciably larger than the theoretical ϵ from Poisson sampling.

quires more than 10^9 observations to converge (we do not explore beyond 10^9 due to computational constraints). Recall that we audit using the (ϵ, δ) -DP definition because the privacy loss distribution (PLD) used in [43] is not currently known for DP-SGD (Shuffle).

As expected, given enough observations, our audits match the theoretical lower bounds calculated by Chua et al. [16] but do not exceed it. This not only confirms that our auditing procedure is effective but also that it might be possible to convert [16]’s *lower-bound privacy analysis* into an *upper-bound privacy guarantee*. However, proving upper-bound privacy guarantees might not be trivial and is beyond our scope; thus, we leave it to future work.

6.2.2 Exploring realistic parameter settings

Next, we audit realistic parameter settings used in state-of-the-art differentially private models. Specifically, we audit BGM in the settings used in [19] and [40] to train private image classification models and large language models, respectively. This corresponds to auditing DP-SGD (Shuffle) under the Worst-Case threat model. Note that De et al. [19] explicitly state they train their models with shuffling but report DP guarantees as though Poisson sampling was used. Whereas, Li et al. [40] do not mention using shuffling, but a review of their codebase shows they use the default Pytorch implementation of DataLoader, which shuffles the dataset.

In total, we audit all 101 combinations of parameters (i.e., noise multiplier, σ , number of steps per epoch, T , and number of epochs E) extracted from [19] and [40] using 10^7 observations. Overall, we find a substantial gap between the empirical privacy leakage under shuffling and the theoretical Poisson analysis in two-thirds of the settings studied. In Table 1, we report the settings with the maximum gaps ($\frac{\epsilon_{emp}}{\epsilon}$) for each dataset used in prior work. The largest gap ($4.25\times$) occurs with large language models, probably owing to the small noise multiplier used to optimize utility.

6.3 Auditing DP-SGD (Shuffle)

Next, we audit DP-SGD (Shuffle) under the Partially-Informed threat model described in Section 5.1 (unless otherwise stated). In all experiments, we use a randomly sampled gradient from the unit ball as the canary gradient, although we did not notice any significant difference

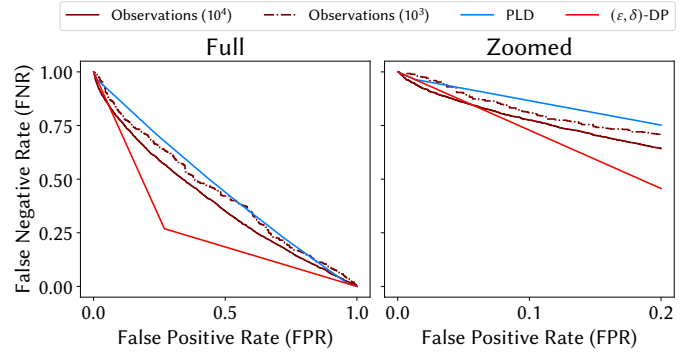


Figure 4: Comparison of tradeoff curves between our observations from auditing DP-SGD (Shuffle) (95% Clopper-Pearson upper bound) at theoretical $\epsilon = 1.0$ and the corresponding theoretical tradeoff curves from (ϵ, δ) -DP and from the PLD analysis of DP-SGD (Poisson). The plot on the right is zoomed in on $0 \leq \text{FPR} \leq 0.2$.

between different types of canary gradients (e.g., dirac) in preliminary experiments.

6.3.1 Comparing trade-off curves

We begin by auditing a CNN model on CIFAR-10 for one epoch using shuffling with batch size $B = 100$ and calibrate the noise multiplier to satisfy $\epsilon = 1.0$ if Poisson sub-sampling was used.

In Figure 4, we plot the FPR-FNR curve (95% Clopper-Pearson upper bound) from training 10^3 , 10^4 models and the curves for the corresponding theoretical (ϵ, δ) -DP at $\epsilon = 1.0$ and PLD bounds expected if Poisson sub-sampling had been used. We note that an *upper bound* on FPR and FNR is used to compute the corresponding *lower bound* on empirical ϵ_{emp} as explained previously in Section 3.2. Due to computational constraints, we are only able to train 10^4 models for this experiment.

We find substantial gaps regardless of the number of observations. More precisely, even a relatively small number of observations (10^3) is enough to detect that the DP-SGD (Shuffle) implementation violates the theoretical privacy guarantees provided by the Poisson sub-sampling analysis. However, while auditing with the PLD curve would allow an adversary to identify that a given implementation of DP-SGD did not specifically use Poisson sub-sampling, it may not necessarily mean that the underlying implementation does not satisfy (ϵ, δ) -DP in general.

To estimate the empirical privacy leakage observed from DP-SGD (Shuffle), we would need to audit using the (ϵ, δ) -DP definition instead. In Figure 4, this would correspond to comparing the observed FPR-FNR curves with the (ϵ, δ) -DP curve instead ($\epsilon = 1.0$). Here, there is a much smaller gap, with the trade-off curve for 10^4 observations only violating (ϵ, δ) -DP at FPRs < 0.05 , and the trade-off curve for 10^3 not violating the theoretical DP guarantees at all. Therefore, 10^3 observations are not enough to detect a violation of (ϵ, δ) -DP guarantee: the violation can only be detected by using at least 10^4 observations at very low FPRs.

Impact of CIs. To better understand the dependence on the

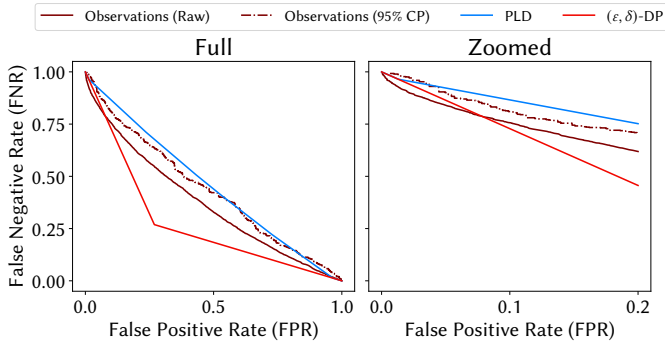


Figure 5: Comparison of tradeoff curves between our 10^3 observations from auditing DP-SGD (Shuffle) (Raw vs. 95% CP upper bound) and the theoretical tradeoff curves from (ϵ, δ) -DP and PLD analysis for DP-SGD (Poisson). Plot on the right is zoomed in on $0 \leq \text{FPR} < 0.2$.

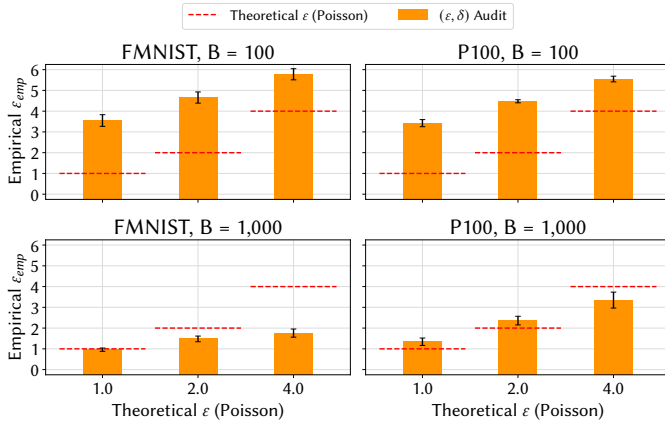


Figure 6: Auditing DP-SGD (Shuffle) at various batch sizes B and privacy levels ϵ .

number of observations, we also analyze the impact of using Clopper-Pearson (CP) CIs. In Figure 5, we plot the tradeoff curves from the same experiment with 10^3 observations with and without the CP upper bounds. We notice a large gap between the “raw” observed trade-off curve (w/o CP upper bounds) and the trade-off curve with CP upper bounds. Specifically, when using the trade-off curve with CP bounds, we estimate a lower bound ϵ_{emp} , which is always numerically smaller than the ϵ_{emp} estimated from the “raw” trade-off curve, thus making it more difficult to detect violations of (ϵ, δ) -DP.

Nevertheless, in DP auditing, we are interested not only in estimating the empirical privacy leakage but also in the associated confidence level. This allows us to reduce false positives and provide assurances that the privacy violations are real, especially when debugging implementations (as we do later in Section 7). As a result, we believe it necessary to use CP intervals in our auditing experiments, even though that requires more training runs.

6.3.2 Varying batch size B and theoretical ϵ

Next, we evaluate the impact of the batch size and theoretical (Poisson) ϵ on the empirical privacy leakage observed from

DP-SGD (Shuffle) under Partially-Informed. Due to computational constraints, rather than a CNN on CIFAR-10, we audit a LeNet model on FMNIST and an MLP model on P100 over 10^6 observations. In Figure 6, we plot the empirical leakage estimates ϵ_{emp} observed from auditing DP-SGD (Shuffle) at various batch sizes and privacy levels ϵ .

With $B = 100$, the empirical privacy leakage is significantly larger than the theoretical guarantees across both datasets and privacy levels. Specifically, for $B = 100$ and theoretical $\epsilon = 1.0, 2.0, 4.0$, the models trained on FMNIST and P100 had empirical privacy guarantees of $\epsilon_{emp} = 3.46, 4.66, 5.78$ and $3.42, 4.48, 5.55$, respectively.

However, with a larger batch $B = 1000$, we only detect small gaps in some settings. Under Partially-Informed, the gradients of all samples remain unchanged except for the target record and final record in each batch. Thus, this likely introduces a “bias” term when evaluating the output from each step, i.e., $o_t^i \leftarrow \langle \hat{g}, \hat{g} \rangle$. Although Nasr et al. [43] show that this bias does not affect audits of DP-SGD (Poisson), they simply threshold the output from each step. Our auditing procedure is more complicated as we compute a likelihood ratio function across multiple steps, which we believe is more susceptible to the bias term thus resulting in weaker audits than expected from BGM. However, in several settings, the empirical privacy leakage is close to or already exceeds the theoretical Poisson guarantee, suggesting that given enough observations ($\approx 10^9$), we can potentially detect larger. Due to computational constraints, we leave this as part of future work.

6.3.3 Varying adversarial capabilities

Our experiments thus far have shown that auditing DP-SGD (Shuffle) under Partially-Informed reveals large gaps between the empirical privacy leakage observed and the theoretical guarantees promised by the Poisson sub-sampling analysis. However, Partially-Informed is a stronger threat model than typically used in prior work [43]. Consequently, we set out to evaluate the impact of adversarial capabilities on the empirical privacy leakage observed.

In Figure 7, we report the empirical privacy leakage estimates ϵ_{emp} when auditing DP-SGD (Shuffle) under the three different threat models. We fix the batch size to $B = 100$ and use 10^6 observations. Despite the “bias” from other training samples discussed above, the empirical privacy leakage under Partially-Informed is almost the same as that from the idealized Worst-Case threat model (which corresponds to auditing BGM) at small batch sizes. Specifically, on FMNIST, at $\epsilon = 1.0, 2.0, 4.0$, auditing under Partially-Informed and Worst-Case yield privacy leakage estimates of $\epsilon_{emp} = 3.55, 4.66, 5.78$ and $\epsilon_{emp} = 4.06, 5.18, 6.43$, respectively.

However, estimates under Natural are significantly weaker than the other two threat models. In all settings, ϵ_{emp} under Natural is actually smaller than the theoretical ϵ guaranteed by Poisson sub-sampling, even though shuffling was used. This is because the negative canary gradients inserted by the Partially-Informed adversary are crucial in “identifying” the batch containing the target (or zero-out) record in each epoch. Specifically, in the Partially-Informed threat

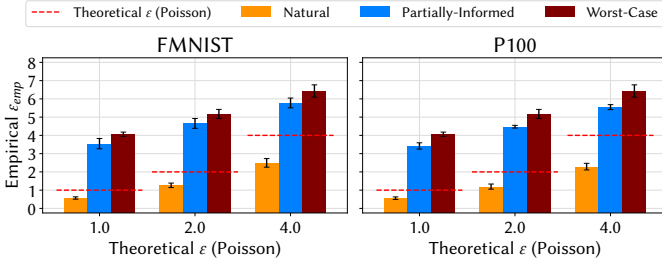


Figure 7: Auditing DP-SGD (Shuffle) under various threat models.

model, without any noise, the adversary aims to distinguish between $(-1, \dots, +1, \dots, -1)$ and $(-1, \dots, 0, \dots, -1)$, which has a Hamming distance of 2 with high probability (assuming the ‘+1’ and ‘0’ appear in different batches). Whereas under Natural, they have to distinguish between $(0, \dots, +1, \dots, 0)$ and $(0, \dots, 0)$, which only has a Hamming distance of 1. Informally, the distributions of outputs observed under Natural are less distinguishable than under Partially-Informed, thus resulting in lower empirical privacy leakage estimates.

6.4 Main Takeaways

Our experiments show that the empirical privacy leakage from shuffling is substantially larger than the theoretical guarantees stemming from the Poisson sub-sampling analysis. This gap occurs in a wide range of parameter settings studied and, crucially, in those used to train SOTA as well [19, 40]. For instance, De et al. [19] reportedly use shuffling to fine-tune a NF-ResNet-50 model on the Places-365 dataset at a theoretical $\epsilon = 7.53$, but our audits show that the actual privacy leakage is almost double ($\epsilon_{emp} = 13.59$).

We also show that the gap is also observable when auditing real models trained using the DP-SGD (Shuffle) algorithm. Specifically, when auditing a LeNet-5 classifier trained on the FMNIST dataset at theoretical $\epsilon = 1.0$ under the slightly weaker Partially-Informed threat model, we observe an empirical $\epsilon_{emp} = 3.46$, almost $3.5\times$ the theoretical guarantee. However, under the weakest threat model considered, i.e., Natural, the ϵ_{emp} is often below the expected theoretical guarantees ϵ , which suggests that strong threat models are necessary to audit shuffling mechanisms effectively.

7 Debugging Shuffle Implementations

Implementing DP algorithms correctly is known to be challenging [10, 34], and DP violations have been found in the wild [4, 54]. Specific to shuffling, Ponomareva et al. [49] report that for computational reasons, in many cases, datasets may not even be shuffled fully but only within a small buffer. Therefore, bugs or variations to the shuffling procedure itself may be present in DP-SGD implementations used in the wild, and, naturally, this would substantially affect their privacy leakage.

Based on a search of public GitHub code repositories (see Section 7.2), we identify cases where the dataset is first batched, and the batches are then shuffled instead of shuffling

Algorithm 2 Auditing Partial Shuffling (with Buffer K)

Require: Dataset, D . Number of observations, N . Target record, (\hat{x}, \hat{y}) . Zero-out record, (x_{\perp}, y_{\perp}) . Significance level, α . Privacy parameter, δ .

```

1: for  $i \in [\frac{N}{2}]$  do
2:    $\Theta[i] \leftarrow \text{DP-SGD}_K^{\text{PI}}(\{(\hat{x}, \hat{y})\} \cup D; -)$ 
3:    $\Theta'[i] \leftarrow \text{DP-SGD}_K^{\text{PI}}(\{(x_{\perp}, y_{\perp})\} \cup D; -)$ 
4: for  $k \in \{1, 10, 20, \dots, 100\}$  do
5:   for  $i \in [\frac{N}{2}]$  do
6:      $[\mathbf{o}_1 | \dots | \mathbf{o}_T] \leftarrow \Theta[i]$ 
7:      $[\mathbf{o}'_1 | \dots | \mathbf{o}'_T] \leftarrow \Theta'[i]$ 
8:      $\mathcal{S}[i] \leftarrow \Lambda^{\text{PI}}([\mathbf{o}_1 | \dots | \mathbf{o}_k])$ 
9:      $\mathcal{S}'[i] \leftarrow \Lambda^{\text{PI}}([\mathbf{o}'_1 | \dots | \mathbf{o}'_k])$ 
10:   $\epsilon_{emp}[k] \leftarrow \text{EstimateEps}(\mathcal{S}, \mathcal{S}', \alpha, \delta)$ 
11: return  $\max_k \epsilon_{emp}[k]$ .
```

the samples before batching. As visualized in Appendix D.2, this makes the batch with the target record substantially more identifiable in cases where the samples surrounding it are different from samples “far away” from it (in this setting, batching is done locally). While these variations to the shuffling procedure intuitively affect the privacy analysis, in this section, we verify whether our auditing procedure can identify them and determine the scale of their impact on privacy leakage.

7.1 Partial Shuffling

We first consider the case where datasets are only shuffled within a small buffer of K samples, as reported in [49], and report the procedure used to debug this variation in Algorithm 2. The dataset is shuffled in buffers of size K , i.e., the first K samples are shuffled and batched, followed by the next K samples, etc. (See Appendix D.1 for a visualization of a small dataset that is partially shuffled.)

Methodology. We assume the Partially-Informed adversary, where the output remains (mostly) the same at $(-1, \dots, +1, \dots, -1) + \mathcal{N}(0, \sigma^2 \mathbb{I})$ and $(-1, \dots, 0, \dots, -1) + \mathcal{N}(0, \sigma^2 \mathbb{I})$ for D and D' , respectively. However, while in full shuffling, the ‘+1’ and ‘0’ can appear uniformly in any batch, here they can only appear in the first $\lfloor \frac{K}{B} \rfloor$ batches since the first K samples are first shuffled and then batched.

The remaining challenge in identifying this bug is that the adversary does not have access to the batch sampler \mathcal{B} and, by extension, does not know K . We impose this restriction as, even in a real-world auditing setting, it may be cumbersome for an auditor to be given access to the batch sampler separately—even then, the model trainer may not faithfully use the batch sampler. Therefore, we allow the adversary to “guess” multiple buffer sizes and evaluate empirical privacy leakage from only the first K batches. The adversary then outputs the maximum empirical privacy leakage observed across all buffer sizes guessed. Theoretically, they could perform a binary search to reduce the number of guesses made; however, we assume they search over $K = \{1, 10, 20, \dots, 100\}$ since the number of batches is small. Also, in theory, the empirical privacy leakage from each guess must be calculated on sep-

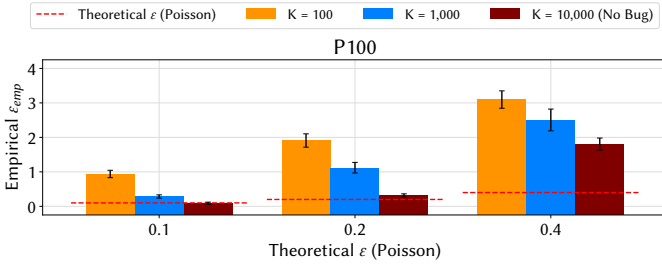


Figure 8: Auditing DP-SGD (Shuffle) when the dataset is only shuffled within a buffer of K samples. When the buffer $K = |D| = 10,000$, the dataset is fully shuffled.

arate sets of observations for the 95% CI to be valid, similar to choosing the optimal threshold. However, to evaluate the maximum empirical privacy leakage achievable, we omit this step and instead report standard deviations over five runs.

We review the procedure used to debug this variation in Algorithm 2. We denote with DP-SGD_K^{PI} the execution of DP-SGD with partial shuffle over a buffer of size K and with the modifications made for the Partially-Informed adversary as in Algorithm 1.

Results. In Figure 8, we report the empirical privacy leakage estimates for various buffer sizes K . We only audit the MLP model trained on P100 due to computational constraints. We experiment with small $\epsilon = 0.1, 0.2, 0.4$ as the violations are much more significant in this regime. Specifically, at $\epsilon = 0.1, 0.2, 0.4$, the empirical privacy leakages for full dataset shuffling $K = 10,000$ and partial shuffling at $K = 1,000$ are $\epsilon_{emp} = 0.09, 0.31, 1.80$ and $\epsilon_{emp} = 0.29, 1.12, 2.51$, respectively. This shows that even partial shuffling can result in substantially larger empirical privacy leakages.

However, as ϵ increases, the gap between full shuffling and no shuffling ($K = 100$) reduces. For instance, at $\epsilon = 0.1, 0.2, 0.4$, the ϵ_{emp} values from no shuffling are $10.4\times$, $6.16\times$, and $1.72\times$ that of the ϵ_{emp} values from full shuffling, respectively. This indicates that for larger values of ϵ , the impact of not shuffling or partial shuffling steadily decreases, which in turn suggests that shuffling may not always result in strong privacy amplification.

7.2 Batch-then-Shuffle

Finally, we debug the variation where a dataset is first batched and then shuffled. Although this is not necessarily a known bug in the context of training private models, we find a substantial presence of this sequence of events in public repositories related to non-private ones. Specifically, we use the GitHub Code Search tool to search for occurrences of `dataset.batch(*).shuffle(*)`, which indicates that the dataset is first batched before it is shuffled, and compare with occurrences of `dataset.shuffle(*).batch(*)`.

We find approximately 10,800 files using the “correct” shuffle-then-batch implementation and 290 files (2.6%) using the batch-then-shuffle approach. As a result, we set out to preemptively explore techniques to catch these bugs.

Under the Natural and Partially-Informed threat models,

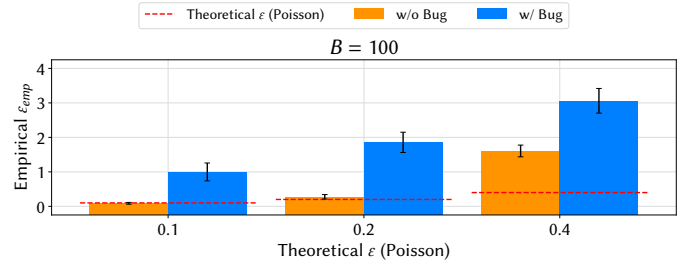


Figure 9: Auditing DP-SGD (Shuffle) when the dataset is batched before shuffling is performed.

batch-then-shuffle is equivalent to shuffle-then-batch. This is because we expect the dot product of the privatized gradient and gradient of almost all other samples, which cannot be modified by the adversary, to be near 0 under both threat models. Thus, this bug can only be detected under the Worst-Case threat model.

We then consider the Worst-Case threat model, but we let the adversary insert the gradients of the first B samples as the canary gradient \hat{g} and the remaining samples as the negative canary gradient $-\hat{g}$. By doing so, the outputs from the DP-SGD algorithm are expected to be $(B, -B, \dots, -B) + \mathcal{N}(0, \sigma^2 \mathbb{I})$ and $(B-1, -B, \dots, -B) + \mathcal{N}(0, \sigma^2 \mathbb{I})$ for D and D' , respectively. Note that ‘ B ’ and ‘ $B-1$ ’ can appear uniformly in any batch. (See Appendix D.2 for a visualization of a small dataset that is batched first and then shuffled.)

We adjust the likelihood ratio used under the Worst-Case threat model accordingly and report the audit results with/without the bug in Figure 9. Our audit can indeed easily detect this bug: at $\epsilon = 0.1, 0.2, 0.4$, $\epsilon_{emp} = 1.00, 1.86, 3.06$, respectively, with the bug but only $\epsilon_{emp} = 0.09, 0.28, 1.61$, respectively, without the bug.

7.3 Take-aways

The analysis presented in this section shows that our auditing procedure is highly extensible as it can be used to audit common variations of the shuffling procedure, more precisely, “partial shuffling” and “batch-then-shuffle.”

We show that these variations remain easily detectable by our auditing method, which estimates $\epsilon_{emp} = 0.29, 1.12, 2.51$ and $\epsilon_{emp} = 1.00, 1.86, 3.06$ for the “partial shuffling” and “batch-then-shuffle” procedure at theoretical $\epsilon = 0.1, 0.2, 0.4$, respectively.

8 Related Work

To our knowledge, we are the first to audit DP-SGD with shuffling. In the following, we review relevant prior work on shuffling and auditing DP-SGD.

DP-SGD Audits. Jayaraman et al. [33] present the first DP-SGD audit using black-box inference attacks on the final trained model but only achieve loose estimates of the privacy leakage. Jagielski et al. [32] use input canaries to improve tightness and use Clopper-Pearson intervals to calculate confidence intervals for the empirical estimates. Nasr et al. [44] are the first

to achieve tight DP-SGD audits using a large number of training runs, a pathological dataset, and an active white-box adversary that can insert gradient canaries at each step. To reduce the number of training runs, Zanella-Béguelin et al. [61] use credible intervals instead of Clopper-Pearson. Although [43] later questions the validity of the credible intervals, it shows that tight empirical estimates are possible even with few training runs and natural (not adversarially crafted) datasets by auditing with f -DP. Recent work on DP-SGD audits has also focused on federated learning settings [2, 41] and further reducing the number of training runs [48] to a single one [2, 42, 52] and auditing under weak threat models [3, 11].

Overall, prior work auditing DP-SGD implementations has focused on Poisson sub-sampling. Previous audits also typically threshold the losses [3, 32, 42, 43, 44, 48, 52] or gradients [42, 43, 44, 44, 48] directly. By contrast, we audit the shuffling setting and use likelihood ratio functions to audit DP-SGD.

Shuffling and DP-SGD. To the best of our knowledge, there is limited prior work analyzing the privacy of DP-SGD with shuffling. Chua et al. [16] analyze a simplified version of DP-SGD, i.e., the Adaptive Batch Linear Query (ABLQ) mechanism. Although they do not present a theoretical upper bound for the ABLQ mechanism with shuffling, they consider pathological settings where ABLQ could leak more privacy when using shuffling instead of Poisson sub-sampling. While they initially only consider a single epoch [16], in follow-up work [17], they extend their lower bound to multiple epochs. However, neither work directly analyzes DP-SGD or evaluates the gap in real-world parameter settings.

Our work takes a different approach, empirically estimating the privacy leakage from DP-SGD using DP auditing. By doing so, we derive empirical privacy leakage estimates for real-world models trained using DP-SGD (Shuffle). We also focus on the impact of real-world considerations like threat models and variations on the shuffling procedure, which Chua et al. [16] mention would require more careful analysis but leave to future work.

Shuffling. Shuffling is also used in other areas of DP, e.g., local DP, where users first randomize their inputs before submitting them for data processing. Bittau et al. [8] present the “Encode-Shuffle-Analyze” (ESA) framework where users’ randomized samples are shuffled before being processed. Erlingsson et al. [26] and Cheu et al. [12] formally prove that shuffling users’ data improves privacy guarantees in the local DP setting. Balle et al. [6] then improve on and generalize results from [26]. Erlingsson et al. [25] later revisit and apply their privacy amplification results to the ESA framework. More recently, Feldman et al. [27, 28] and Wang et al. [55] present a nearly optimal analysis of shuffling in the local DP setting. Overall, the privacy analysis for (ϵ, δ) -DP mechanisms typically used in central DP is far less understood than that of shuffling for local DP mechanisms, which typically guarantee pure DP (i.e., $\delta = 0$).

9 Conclusion

This paper presented the first audit of DP-SGD implementations that use shuffling but report DP guarantees as though Poisson sub-sampling was used, investigating the differences between the theoretical guarantees of the latter and the empirical privacy leakage from the former. We did so as using shuffling to sample batches in DP-SGD has become common practice [19, 40, 49] as it is much more computationally efficient.

We introduced new auditing techniques and audited DP-SGD (Shuffle) under varying parameter settings and threat models. Our experiments revealed, even in real-world settings, a substantial gap between the empirical privacy leakage observed from DP-SGD (Shuffle) and the theoretical guarantees of DP-SGD (Poisson). More precisely, we experimented with 101 settings from SOTA models using shuffling [19, 40], finding substantial gaps in two-thirds of them. We also discussed how these gaps can depend on the batch size used and the threat model, with smaller batch sizes and stronger threat models resulting in larger gaps.

Finally, we showed that our auditing techniques can be used to detect the presence of bugs in the implementations of the shuffling procedure. We investigated two common bugs [49] found in public code repositories of non-private model training, showing that our auditing framework effectively identifies them and detects even higher empirical privacy leakages in the presence of these bugs.

Implications. The measurable difference between the empirical privacy leakage observed from DP-SGD (Shuffle) and the theoretical guarantees of DP-SGD (Poisson) shows that prior work [19, 40] substantially overestimated the privacy guarantees of SOTA private models. In some instances, the actual privacy leakage is more than $4\times$ greater than the theoretical DP guarantees.

Consequently, our work calls into question the validity of theoretical guarantees and prompts the need to formally analyze the privacy guarantees provided by shuffling the dataset. Our analysis also attests to the dangers of making seemingly simple modifications to provably correct DP algorithms.

Threat Models. Our analysis considers active white-box threat models when auditing DP-SGD (Shuffle). Specifically, we assume that the adversary can insert a target sample of their choice and view the final trained model and that they can insert (varying sizes of) canary gradients at each step and observe all intermediate models. Although the adversaries may not always have these capabilities in real-world settings, we emphasize that the provably correct DP guarantees are meant to be robust against *worst-case* adversaries, making them valid in the context of auditing. In fact, the same assumptions were made in prior DP-SGD audits [43, 44].

Interestingly, we detected significant differences in empirical privacy leakages depending on the threat models we experimented with. This suggests that the empirical privacy leakage for DP-SGD (Shuffle) may be lower under weaker/more realistic threat models – similar to findings from prior work

for DP-SGD (Poisson) [15, 29, 45, 59]. Therefore, investigating whether the empirical privacy leakage from DP-SGD (Shuffle) exceeds the guarantees provided by DP-SGD (Poisson) even under weaker threat models would be an interesting future direction.

Future Work. In future work, we plan to minimize the number of training runs required to audit DP-SGD (Shuffle) accurately. Recent work presented methods to audit DP-SGD (Poisson) with just one training run [2, 42, 48, 52]. However, these techniques may not directly apply to DP-SGD (Shuffle) and currently underestimate the privacy leakage even under power threat models, requiring substantial effort to adapt to our setting. Furthermore, our audits are currently weaker for larger batch sizes, which we believe is mainly due to the bias introduced by the “other” samples. Therefore, we also plan to reduce this bias term using debiasing techniques that can enable our audits to be effective even for large batch sizes.

References

- [1] M. Abadi, A. Chu, I. Goodfellow, H. B. McMahan, I. Mironov, K. Talwar, and L. Zhang. Deep Learning with Differential Privacy. In *CCS*, 2016.
- [2] G. Andrew, P. Kairouz, S. Oh, A. Oprea, H. B. McMahan, and V. Suriyakumar. One-shot Empirical Privacy Estimation for Federated Learning. In *ICLR*, 2024.
- [3] M. S. M. S. Annamalai and E. De Cristofaro. Nearly Tight Black-Box Auditing of Differentially Private Machine Learning. In *NeurIPS*, 2024.
- [4] M. S. M. S. Annamalai, G. Ganey, and E. De Cristofaro. “What do you want from theory alone?” Experimenting with Tight Auditing of Differentially Private Synthetic Data Generation. In *USENIX Security*, 2024.
- [5] B. Balle, G. Barthe, and M. Gaboardi. Privacy Amplification by Subsampling: Tight Analyses via Couplings and Divergences. In *NeurIPS*, 2018.
- [6] B. Balle, J. Bell, A. Gascón, and K. Nissim. The Privacy Blanket of the Shuffle Model. In *CRYPTO*, 2019.
- [7] B. Balle, L. Berrada, S. De, S. Ghalebiksebi, J. Hayes, A. Pappu, S. L. Smith, and R. Stanforth. JAX-Privacy: Algorithms for Privacy-Preserving Machine Learning in JAX. <https://github.com/google-deeppmind/jax-privacy>, 2022.
- [8] A. Bittau, Ú. Erlingsson, P. Maniatis, I. Mironov, A. Raghunathan, D. Lie, M. Rudominer, U. Kode, J. Tinnes, and B. Seefeld. Prochlo: Strong Privacy for Analytics in the Crowd. In *SOPS*, 2017.
- [9] N. Carlini, S. Chien, M. Nasr, S. Song, A. Terzis, and F. Tramèr. Membership Inference Attacks From First Principles. In *IEEE S&P*, 2022.
- [10] T. Cebere. Privacy Leakage at low sample size. <https://github.com/pytorch/opacus/issues/571>, 2023.
- [11] T. Cebere, A. Bellet, and N. Papernot. Tighter Privacy Auditing of DP-SGD in the Hidden State Threat Model. *arXiv:2405.14457*, 2024.
- [12] A. Cheu, A. Smith, J. Ullman, D. Zeber, and M. Zhilyaev. Distributed Differential Privacy via Shuffling. In *Eurocrypt*, 2019.
- [13] C. A. Choquette-Choo, A. Ganesh, S. Haque, T. Steinke, and A. Thakurta. Near Exact Privacy Amplification for Matrix Mechanisms. *arXiv:2410.06266*, 2024.
- [14] C. A. Choquette-Choo, A. Ganesh, R. McKenna, H. B. McMahan, J. Rush, A. Guha Thakurta, and Z. Xu. (Amplified) Banded Matrix Factorization: A unified approach to private training. In *NeurIPS*, 2024.
- [15] R. Chourasia, J. Ye, and R. Shokri. Differential Privacy Dynamics of Langevin Diffusion and Noisy Gradient Descent. *NeurIPS*, 2021.
- [16] L. Chua, B. Ghazi, P. Kamath, R. Kumar, P. Manurangsi, A. Sinha, and C. Zhang. How Private are DP-SGD Implementations? In *ICML*, 2024.
- [17] L. Chua, B. Ghazi, P. Kamath, R. Kumar, P. Manurangsi, A. Sinha, and C. Zhang. Scalable DP-SGD: Shuffling vs. Poisson Subsampling. *arXiv:2411.04205*, 2024.
- [18] C. J. Clopper and E. S. Pearson. The use of confidence or fiducial limits illustrated in the case of the binomial. *Biometrika*, 1934.
- [19] S. De, L. Berrada, J. Hayes, S. L. Smith, and B. Balle. Unlocking High-Accuracy Differentially Private Image Classification through Scale. *arXiv:2204.13650*, 2022.
- [20] E. Debenedetti, G. Severi, N. Carlini, C. A. Choquette-Choo, M. Jagielski, M. Nasr, E. Wallace, and F. Tramèr. Privacy Side Channels in Machine Learning Systems. In *USENIX*, 2024.
- [21] Z. Ding, Y. Wang, G. Wang, D. Zhang, and D. Kifer. Detecting Violations of Differential Privacy. In *CCS*, 2018.
- [22] J. Dong, A. Roth, and W. J. Su. Gaussian Differential Privacy. *arXiv:1905.02383*, 2019.
- [23] F. Dörmann, O. Frisk, L. N. Andersen, and C. F. Pedersen. Not All Noise is Accounted Equally: How Differentially Private Learning Benefits from Large Sampling Rates. In *MLSP*, 2021.
- [24] C. Dwork, F. McSherry, K. Nissim, and A. Smith. Calibrating Noise to Sensitivity in Private Data Analysis. In *TCC*, 2006.
- [25] Ú. Erlingsson, V. Feldman, I. Mironov, A. Raghunathan, S. Song, K. Talwar, and A. Thakurta. Encode, Shuffle, Analyze Privacy Revisited: Formalizations and Empirical Evaluation. *arXiv:2001.03618*, 2020.
- [26] Ú. Erlingsson, V. Feldman, I. Mironov, A. Raghunathan, K. Talwar, and A. Thakurta. Amplification by Shuffling: From Local to Central Differential Privacy via Anonymity. In *SODA*, 2019.
- [27] V. Feldman, A. McMillan, and K. Talwar. Hiding Among the Clones: A Simple and Nearly Optimal Analysis of Privacy Amplification by Shuffling. In *FOCS*, 2022.
- [28] V. Feldman, A. McMillan, and K. Talwar. Stronger Privacy Amplification by Shuffling for Renyi and Approximate Differential Privacy. In *SODA*, 2023.
- [29] V. Feldman, I. Mironov, K. Talwar, and A. Thakurta. Privacy Amplification by Iteration. In *IEEE Symposium on Foundations of Computer Science*, 2018.
- [30] V. Feldman and M. Shenfeld. Privacy amplification by random allocation. *arXiv:2502.08202*, 2025.
- [31] Google. TensorFlow Privacy. <https://github.com/tensorflow/privacy>, 2019.
- [32] M. Jagielski, J. Ullman, and A. Oprea. Auditing Differentially Private Machine Learning: How Private is Private SGD? In *NeurIPS*, 2020.
- [33] B. Jayaraman and D. Evans. Evaluating differentially private machine learning in practice. In *USENIX Security*, 2019.
- [34] M. Johnson. Fix prng key reuse in differential privacy example. <https://github.com/google/jax/pull/3646>, 2020.
- [35] P. Kairouz, B. McMahan, S. Song, O. Thakkar, A. Thakurta, and Z. Xu. Practical and Private (Deep) Learning Without Sampling or Shuffling. In *ICML*, 2021.
- [36] P. Kairouz, S. Oh, and P. Viswanath. The Composition Theorem for Differential Privacy. In *ICML*, 2015.
- [37] A. Koskela, J. Jälkö, and A. Honkela. Computing Tight Differential Privacy Guarantees Using FFT. In *AISTATS*, 2020.

- [38] A. Krizhevsky. Learning Multiple Layers of Features from Tiny Images. <https://www.cs.utoronto.ca/~kriz/learning-features-2009-TR.pdf>, 2009.
- [39] Y. LeCun, L. Bottou, Y. Bengio, and P. Haffner. Gradientbased learning applied to document recognition. *Proceedings of the IEEE*, 86(11), 1998.
- [40] X. Li, F. Tramèr, P. Liang, and T. Hashimoto. Large Language Models Can Be Strong Differentially Private Learners. In *ICLR*, 2022.
- [41] S. Maddock, A. Sablayrolles, and P. Stock. CANIFE: Crafting Canaries for Empirical Privacy Measurement in Federated Learning. In *ICLR*, 2023.
- [42] S. Mahloui, L. Melis, and K. Chaudhuri. Auditing f -Differential Privacy in One Run. *arXiv:2410.22235*, 2024.
- [43] M. Nasr, J. Hayes, T. Steinke, B. Balle, F. Tramèr, M. Jagielski, N. Carlini, and A. Terzis. Tight Auditing of Differentially Private Machine Learning. In *USENIX Security*, 2023.
- [44] M. Nasr, S. Songi, A. Thakurta, N. Papernot, and N. Carlini. Adversary Instantiation: Lower Bounds for Differentially Private Machine Learning. In *IEEE S&P*, 2021.
- [45] M. Nasr, T. Steinke, A. Ganesh, B. Balle, C. A. Choquette-Choo, M. Jagielski, J. Hayes, A. G. Thakurta, A. Smith, and A. Terzis. The Last Iterate Advantage: Empirical Auditing and Principled Heuristic Analysis of Differentially Private SGD. In *ICLR*, 2025.
- [46] J. Neyman and E. S. Pearson. IX. On the problem of the most efficient tests of statistical hypotheses. *Philosophical Transactions of the Royal Society of London. Series A, Containing Papers of a Mathematical or Physical Character*, 231(694-706):289–337, 1933.
- [47] OpenXLA. XLA (Accelerated Linear Algebra). <https://github.com/openxla/xla>, 2024.
- [48] K. Pillutla, G. Andrew, P. Kairouz, H. B. McMahan, A. Oprea, and S. Oh. Unleashing the Power of Randomization in Auditing Differentially Private ML. In *NeurIPS*, 2024.
- [49] N. Ponomareva, S. Vassilvitskii, Z. Xu, B. McMahan, A. Kurakin, and C. Zhang. How to DP-fy ML: A Practical Tutorial to Machine Learning with Differential Privacy. In *KDD*, 2023.
- [50] A. S. Shamsabadi, G. Tan, T. I. Cebere, A. Bellet, H. Haddadi, N. Papernot, X. Wang, and A. Weller. Confidential-DPproof: Confidential Proof of Differentially Private Training. In *ICLR*, 2024.
- [51] R. Shokri, M. Stronati, C. Song, and V. Shmatikov. Membership Inference Attacks against Machine Learning Models. In *IEEE S&P*, 2017.
- [52] T. Steinke, M. Nasr, and M. Jagielski. Privacy Auditing with One (1) Training Run. In *NeurIPS*, 2024.
- [53] F. Tramèr and D. Boneh. Differentially Private Learning Needs Better Features (or Much More Data). In *ICLR*, 2021.
- [54] F. Tramèr, A. Terzis, T. Steinke, S. Song, M. Jagielski, and N. Carlini. Debugging Differential Privacy: A Case Study for Privacy Auditing. *arXiv:2202.12219*, 2022.
- [55] C. Wang, B. Su, J. Ye, R. Shokri, and W. Su. Unified Enhancement of Privacy Bounds for Mixture Mechanisms via f -Differential Privacy. In *NeurIPS*, 2023.
- [56] Z. Xiang, T. Wang, and D. Wang. Privacy Audit as Bits Transmission:(Im) possibilities for Audit by One Run. In *USENIX Security*, 2025.
- [57] H. Xiao, K. Rasul, and R. Vollgraf. Fashion-MNIST: a Novel Image Dataset for Benchmarking Machine Learning Algorithms. *arXiv:1708.07747*, 2017.
- [58] J. Ye, A. Maddi, S. K. Murakonda, V. Bindschaedler, and R. Shokri. Enhanced Membership Inference Attacks against Machine Learning Models. In *CCS*, 2022.
- [59] J. Ye and R. Shokri. Differentially Private Learning Needs Hidden State (Or Much Faster Convergence). *NeurIPS*, 2022.
- [60] A. Yousefpour, I. Shilov, A. Sablayrolles, D. Testuggine, K. Prasad, M. Malek, J. Nguyen, S. Ghosh, A. Bharadwaj, J. Zhao, et al. Opacus: User-friendly Differential Privacy Library in PyTorch. *arXiv:2109.12298*, 2021.
- [61] S. Zanella-Béguelin, L. Wutschitz, S. Tople, A. Salem, V. Rühle, A. Pavard, M. Naseri, B. Köpf, and D. Jones. Bayesian Estimation of Differential Privacy. In *ICML*, 2023.
- [62] Y. Zhu, J. Dong, and Y.-X. Wang. Optimal Accounting of Differential Privacy via Characteristic Function. In *AISTATS*, 2022.

Algorithm 3 Differentially Private Stochastic Gradient Descent (DP-SGD) [1]

Require: Dataset, D . Epochs, E . Batch Size, B . Learning rate, η . Batch sampler, \mathcal{B} . Loss function, ℓ . Initial model parameters, θ_0 . Noise multiplier, σ . Clipping norm, C .

- 1: $T \leftarrow \lfloor D \rfloor / B$
- 2: **for** $i \in [E]$ **do**
- 3: $\theta_1^i \leftarrow \theta_T^{i-1}$
- 4: Sample batches $B_1, \dots, B_T \leftarrow \mathcal{B}(D, B)$
- 5: **for** $t \in [T]$ **do**
- 6: **for** $(x_j, y_j) \in B_t$ **do**
- 7: $g_j \leftarrow \nabla \ell((x_j, y_j); \theta_t^i)$
- 8: $\bar{g}_j \leftarrow g_j / \max(1, \frac{\|g_j\|_2}{C})$
- 9: $\tilde{g} \leftarrow \frac{1}{B} \left(\sum_j \bar{g}_j + \mathcal{N}(0, C^2 \sigma^2 \mathbb{I}) \right)$
- 10: $\theta_{t+1}^i \leftarrow \theta_t^i - \eta \tilde{g}$
- 11: **return** θ_T^E

Algorithm 4 Batched Gaussian Mechanism (BGM)

Require: Dataset, $D = (x_1, \dots, x_N) \in [-1, +1]^N$. Batch Size, B . Number of epochs, E . Batch sampler, \mathcal{B} . Noise multiplier, σ .

- 1: $T \leftarrow \lfloor D \rfloor / B$
- 2: **for** $i \in [E]$ **do**
- 3: Sample batches $B_1, \dots, B_T \leftarrow \mathcal{B}(D, B)$
- 4: **for** $t \in [T]$ **do**
- 5: $\tilde{g}_t^i \leftarrow \sum_{x_i \in B_t} x_i + \mathcal{N}(0, \sigma^2)$
- 6: **return** $\begin{bmatrix} \tilde{g}_1^1 & \dots & \tilde{g}_T^1 \\ \vdots & \ddots & \vdots \\ \tilde{g}_1^E & \dots & \tilde{g}_T^E \end{bmatrix}$

A Differentially Private Stochastic Gradient Descent (DP-SGD)

In Algorithm 3, we review DP-SGD [1]’s pseudo-code. Then, in Algorithm 4, we report that of Batched Gaussian Mechanism (BGM), a heavily simplified version of DP-SGD adapted from [16] to develop principled tight auditing techniques for shuffling under an idealized setting.

B Estimating ε_{emp} from scores

As discussed in Section 3.3, we audit mechanisms by assigning a scalar “score” to each observation and then find the optimal threshold maximizing the empirical estimates ε_{emp} from these scores as done in prior work [3, 11, 32, 43, 44, 48, 61]. However, we substantially improve the efficiency of this procedure by first sorting the scores in increasing order, as reported in Algorithm 5. This enables us to find the optimal threshold from, potentially, billions of observations without incurring a prohibitive computational cost.

C Model Architectures

In our experiments, we audit several (shallow) Convolutional Neural Networks (CNNs) and an MLP model corresponding

Algorithm 5 Estimating ε_{emp} from scores

Require: Scores from $\mathcal{M}(D)$, \mathcal{S} . Scores from $\mathcal{M}(D')$, \mathcal{S}' . Significance level, α . Privacy parameter, δ .

- ▷ Assume $|\mathcal{S}| = |\mathcal{S}'|$.
- 1: $R \leftarrow |\mathcal{S}|$
- ▷ Initial FPR and FNR for classifying all scores as $s \sim \mathcal{M}(D)$.
- 2: $FPR \leftarrow R$
- 3: $FNR \leftarrow 0$
- 4: **for** $\tau \in \text{sort}(\text{increasing}(\mathcal{S} \cup \mathcal{S}'))$ **do** ▷ Calculate FPR and FNR for classifying score as $s \sim \mathcal{M}(D)$ if $s > \tau$.
- 5: **if** $\tau \in \mathcal{S}$ **then**
- 6: $FNR \leftarrow FNR + 1$
- 7: **else**
- 8: $FPR \leftarrow FPR - 1$
- ▷ Calculate confidence intervals for FPR and FNR.
- 9: $\overline{FPR} \leftarrow \text{Clopper-Pearson}(FPR, R, \alpha)$
- 10: $\overline{FNR} \leftarrow \text{Clopper-Pearson}(FNR, R, \alpha)$
- ▷ Estimate ε_{emp} from Equation 1
- 11: $\varepsilon_{emp}[\tau] = \max \left\{ \ln \left(\frac{1 - \overline{FPR} - \delta}{\overline{FNR}} \right), \ln \left(\frac{1 - \overline{FNR} - \delta}{\overline{FPR}} \right), 0 \right\}$
- 12: **return** $\max_{\tau} \varepsilon_{emp}[\tau]$.

Layer	Parameters
Convolution	32 filters of 3x3, stride 1, padding 1
Convolution	32 filters of 3x3, stride 1, padding 1
Max-Pooling	2x2, stride 2, padding 0
Convolution	64 filters of 3x3, stride 1, padding 1
Convolution	64 filters of 3x3, stride 1, padding 1
Max-Pooling	2x2, stride 2, padding 0
Convolution	128 filters of 3x3, stride 1, padding 1
Convolution	128 filters of 3x3, stride 1, padding 1
Max-Pooling	2x2, stride 2, padding 0
Fully connected	128 units
Fully connected	2 units

Table 2: Shallow CNN model for CIFAR-10 with Tanh activations.

to different datasets. More precisely, for the CIFAR-10 dataset, we use the CNN from Dörmann et al. [23], who make minor modifications to the CNNs previously used by Tramèr and Boneh [53]. For the FMNIST dataset, we use a small LeNet-5 model [39]. Finally, for the P100 dataset, we use an MLP model with 32 hidden neurons and ReLU activations.

Exact model architectures for CIFAR-10 and FMNIST are reported in Tables 2 and 3, respectively.

D Visualizing Shuffle Implementations

D.1 Partial Shuffling

In Figure 10, we visualize the possible shufflings of a small dataset with eight records – including a “target record” x_T – when fully shuffled and when partially shuffled using a buffer $K = 4$. We set batch size $B = 2$, which yields four batches in each run. When fully shuffled, x_T appears randomly in all four batches across multiple runs. However, when par-

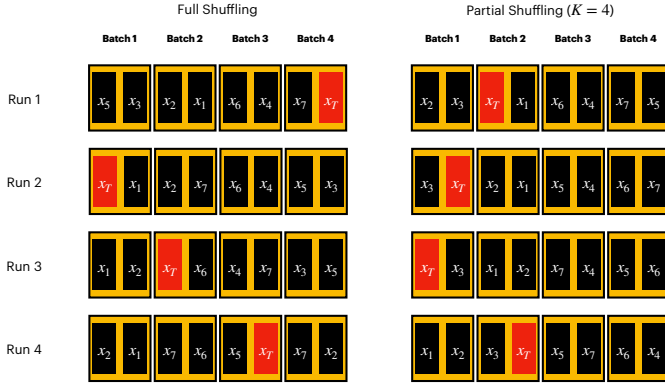


Figure 10: Comparison between a small dataset with eight records being fully shuffled vs. partially shuffled with a buffer of $K=4$ and batch size $B=2$. The target record x_T is highlighted in red.

Layer	Parameters
Convolution	6 filters of 5x5, stride 1, padding 2
Avg-Pooling	2x2
Convolution	16 filters of 5x5, stride 1
Avg-Pooling	2x2
Fully connected	120 units
Fully connected	84 units
Fully connected	2 units

Table 3: LeNet-5 model for FMNIST with Tanh activations.

tially shuffled, x_T can only appear in the first two batches. This means that, in practice, when partially shuffled, the remaining two batches do not provide any extra information to the adversary and can be discarded. Therefore, to audit partial shuffling, the adversary makes “guesses” on the size of the

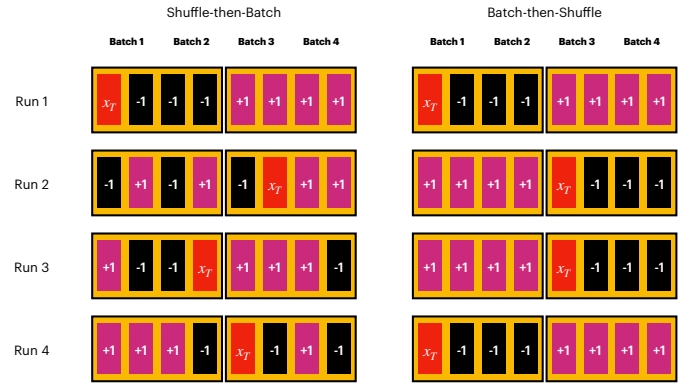


Figure 11: Comparison between a small dataset with 8 records being shuffled then batched (“correct”) vs. batched then shuffled (“wrong”) with batch size $B = 4$. Target record x_T is highlighted in red.

buffer and discards the remaining batches when running the distinguishing function.

D.2 Batch-then-Shuffle

To illustrate the Batch-then-Shuffle setting, we first consider the following one-dimensional dataset $D = (x_T, -1, -1, -1, +1, +1, +1, +1)$ where x_T is the target record. If this dataset is first shuffled and then batched with batch size $B = 4$, each individual ‘-1’ at the beginning and each ‘+1’ at the end of the dataset can appear in either the first or second batch (nearly) independently. However, if the dataset is first batched and the batches are then shuffled, the ‘-1’s at the beginning of the dataset are always grouped together, and similarly, the ‘+1’s at the end. This makes the batch containing the target record much more easily identifiable, as visible from Figure 11.